Applied Thermal Engineering 143 (2018) 701–710

Contents lists available at ScienceDirect

Applied Thermal Engineering

journal homepage: www.elsevier.com/locate/apthermeng

Research Paper

Performance evaluation of a desiccant coated heat exchanger with two different desiccant materials

Turkan Ucok Erkek[a,*], Ali Gungor[a], Hannes Fugmann[b], Alexander Morgenstern[b], Constanze Bongs[b]

[a] Ege University, Engineering Faculty, Department of Mechanical Engineering, 35100 İzmir, Turkey
[b] Fraunhofer Institute for Solar Energy Systems ISE, Heidenhofstraße, 2, 79110 Freiburg, Germany

HIGHLIGHTS

- Simulational analysis of a small-scale desiccant-coated heat exchanger is performed.
- Aluminium fumarate coating is compared with composite silica gel coating.
- Aluminium fumarate coating presents higher loading, sorption capacity values.
- Composite silica gel coating shows better adsorbate mass removal values.

ARTICLE INFO

Keywords:
Desiccant cooling
Desiccant coated heat exchanger
Dehumidification
Heat and mass transfer
Sorption

ABSTRACT

In desiccant cooling systems, the desiccant material reduces the humidity in the process air by removing its moisture. The reduction of the temperature is achieved by heat exchangers, evaporative coolers or conventional cooling coils. These systems draw interest because they allow the use of low quality energy which can support sustainability through energy efficiency.

The desiccant coated heat exchanger is a structure that allows the simultaneous removal of adsorption heat and dehumidification in a single element. This structure is a system element that can contribute extensively to the indoor air humidity control for new generation dehumidification in air conditioning systems. Besides, the dehumidification efficiency of this system has been found to be better than the conventional desiccant wheel. In this study, a desiccant coated small-scale heat exchanger is evaluated by simulation. Silica gel and aluminium fumarate are analysed as desiccant material coatings in this work. Simulations are performed according to two model configurations which are adiabatic and water-cooled cases respectively. Heat and mass transfer characteristics are determined for the two cases as well as the dehumidification and regeneration capacities. The performances of the two materials are compared based on the results of the simulations. Results of the study show the advantages of the water-cooled dehumidification over the adiabatic dehumidification and silica gel composite coating over aluminium fumarate coating.

1. Introduction

The thermal comfort and effects of it on the human being are significant as it is highly related to health, behavior, and productivity [1]. A reasonable degree of thermal comfort can be achieved by controlling indoor air quality parameters such as radiant temperature, air temperature, relative humidity and air velocity. Humidity control is important for several reasons. It is the major part of people's thermal comfort. Besides, when the moisture is over a certain level in a building, this might result in the growth of fungus stirring up problems in air quality. Moreover, moisture removal requires more energy consumption. In humid climates, dehumidification may correspond to a quarter to a third of cooling energy consumption [2].

Solid desiccant materials allow a high capacity of air dehumidification. This phenomenon occurs as a mass transfer process driven by a difference in the vapor pressure in the adsorbed coating layer and the flowing air. Silica gel and lithium chlorides have the most widespread use among commercially available desiccants [3].

Recently, desiccants are proposed to be utilized on coated heat exchangers rather than desiccant wheels to overcome the disadvantages

* Corresponding author.
E-mail address: turkan.ucok.erkek@ege.edu.tr (T.U. Erkek).

https://doi.org/10.1016/j.applthermaleng.2018.06.012
Received 7 October 2017; Received in revised form 22 May 2018; Accepted 3 June 2018
Available online 05 June 2018
1359-4311/

of the release of adsorption heat during the dehumidification process and issues of leakage [4–10].

Weixing et al. [6] proposed a cross-cooled compact solid desiccant dehumidifier which uses silica gel as a desiccant material. The results of the work pointed out that cooled dehumidification by silica gel can strongly enhance the dehumidification performance. Ge et al. [7] declared a novel self-cooled desiccant cooling system based on a desiccant coated heat exchanger (DCHE). This system is introduced to have a cooling power which is by about 30% more than the conventional DCHE cooling system under the stated simulation condition. Bongs et al. [8] presented evaporatively cooled desiccant coated heat exchanger system. According to the findings of the system performance, 46% increase in adsorbed water mass and 4.1-factor improvement of the cooling capacity compared to an air cooled process has been achieved. Hu et al. [9] conducted experiments to determine the performance of a DCHE. The results of the study pointed out a DCHE with a composite desiccant material coating has a higher dehumidification capacity than that of silica gel, and the advantage is more important in low relative humidity conditions. Ge et al. [10] established a mathematical model to determine the performance of a silica gel coated fin-tube heat exchanger cooling system. The results of the simulations show that the operation time is a decisive factor in dehumidification process for the cooling capacity of DCHE system, which can be improved by eliminating the initial period with higher outlet air temperature. Hence, the largest cooling power of this system increase from 2.6 kW to 3.5 kW by eliminating first 50 s of operation time under the summer conditions of Air Conditioning, Heating and Refrigeration Institute.

Tu et al. [11] developed a high-efficiency approach based on a water-adsorbing heat exchanger which makes use of condensation heat and possesses specialties such as compactness and low cost. Experimental results demonstrated that the proposed system had a COP of 6.2 under normal summer conditions according to ISO 5151:1994.

A literature overview reveals that the work has been done so far is currently limited to silica gel as a desiccant material [4–6,8,10,12], except for some research on composite desiccants [9,11,13]. The aim of this study is to analyze the heat and mass transfer characteristics, dehumidification, and regeneration performances of the water-cooled and adiabatic heat exchangers coated with composite silica gel and aluminum fumarate respectively. A simulation model has been constructed and used for this purpose.

2. System description

A schematic figure of a solar driven DCHE cooling system is shown in Fig. 1. A typical system is formed of a cooling system, a heating system, and desiccant coated heat exchanger. Cooling system related to this work is an indirect evaporative cooling system. Heating system is designated as a solar collector or a waste heat source [14–16].

The desiccant coated heat exchanger (DCHE), is the key component of this system which can be in different designs. In this work, for the water-cooled cases, it is a flat tube heat exchanger, and its dimensions are given in Table 1. The schematic of the DCHE is also shown in Fig. 2. Two desiccant coated heat exchangers are designated to work in the system to fulfill the continuous operation conditions of the cooling system. In the first half of the cycle, dehumidification phase-1 occur as air coming from ambient passes through the DCHE 1 (Fig. 1-left). The absolute humidity of the air decreases, while the adsorbent material adsorbes the water. The adsorption heat is removed by means of cooling water passing through the DCHE. In the regeneration phase-1, hot water which is at temperatures in the range of 50 °C to 75 °C is circulated in order to regenerate DCHE 2 (Fig. 1-left). Process air at a high temperature and humidity is released as exhaust air to the environment while the desiccant coating layer is regenerated. At the second half of the cycle, while the dehumidification phase-2 occur in the DCHE 2 (Fig. 1-right), regeneration phase-2 is accomplished in the DCHE 1 (Fig. 1-right).

3. Desiccant materials

The desiccant materials fall into two categories which are solid and liquid. Desiccants such as silica gel, natural zeolite, lithium bromide, lithium chloride, calcium chloride, activated ammonia have a widespread reputation. In this study, silica gel and aluminium fumarate desiccants are used in the simulations.

3.1. Silica gel

Silica gel is an efficient and widely researched material in desiccant wheels by virtue of its good long-term strength, and minimal hysteresis. There are numerous data available in the literature for description and comparison. Nevertheless, its heat-resistancy is not high and therefore it is only convenient for low regeneration temperatures [17]. Each kind of silica gel has only one type of pore, which is generally enveloped in small sized channels. The pore diameters of common silica gel are 2, 3 nm (A type) and 0.7 nm (B type), and the specific surface area is about 100–1000 m^2/g. Silica gel is commonly used for dehumidification because of its high adsorption ability. Type B silica gel is commonly used in conditions where the relative humidity is above 50% whereas Type A silica gel could be used for all dehumidification conditions [18].

In addition, silica gels are currently in use at adsorption heat pumps, and a reasonable amount of work has been carried out to optimize their operation [19]. The silica gel used in this study is silica gel paper composite which is commercially available [21].

Dubinin Astakhov proposed a transformation for equilibrium data which is described in literature [20]. The Dubinin-Astakhov transformation of the equilibrium data for silica gel is shown in Fig. 3, the parameters are reported by [21], see Eq. (1). In Eq. (1), W and A represent the adsorption volume and the adsorption potentials of the silica gel respectively.

$$W = 0.00037237 \bullet \exp^{-\left(\frac{A}{174.39}\right)^{0.92627}} \quad (1)$$

The definitions of adsorption volume and adsorption potential can obtained from the following literature [22,23].

3.2. Aluminium fumarate

Metal organic frameworks draw many interests due to its open crystalline structure and high surface area. Some researchers presented a large capacity of water adsorption within the range of functional use [24–26].

Microporous aluminium fumarate is a metal organic framework (MOF) of which a water uptake of 0.35 g/g is declared at $P/P_{sat} = 0.4$ [19]. Adsorption Isotherm curves of aluminium fumarate for 25, 40 and 60 °C are given in Fig. 4 [27]. Adsorption is proclaimed to occur at $P/P_{sat} = 0.2$ to 0.25 (1.2 kPa), desorption at $P/P_{sat} = 0.45$ to 0.3 (5.6 kPa) under realistic, isobaric working condition. No loss of water capacity has been reported after 40 cycles. These specialties superiorly suit the requirements of thermally driven chillers [19]. A recent study on a microporous aluminium fumarate coated full-scale heat exchanger has shown that a gross cooling power of 2.9 kW or an average cooling power of 0.69 kW (valid until 90% equilibrium loading in 420 s) can be obtained under the working conditions of a realistic adsorption chiller of 90 °C − 30 °C − 18 °C , which are heat source temperature, condenser and evaporator temperature respectively [28].

In this study, aluminium fumarate is preferred because of its availability by cost-effective synthesis.

The Dubinin-Astakhov transformation of the equilibrium data for aluminium fumarate is shown in Fig. 5, the parameters are reported by [29], see Eq. (2).

$$W = 0.00044218 \bullet \exp^{-\left(\frac{A}{185.23}\right)^{2.5}} \quad (2)$$

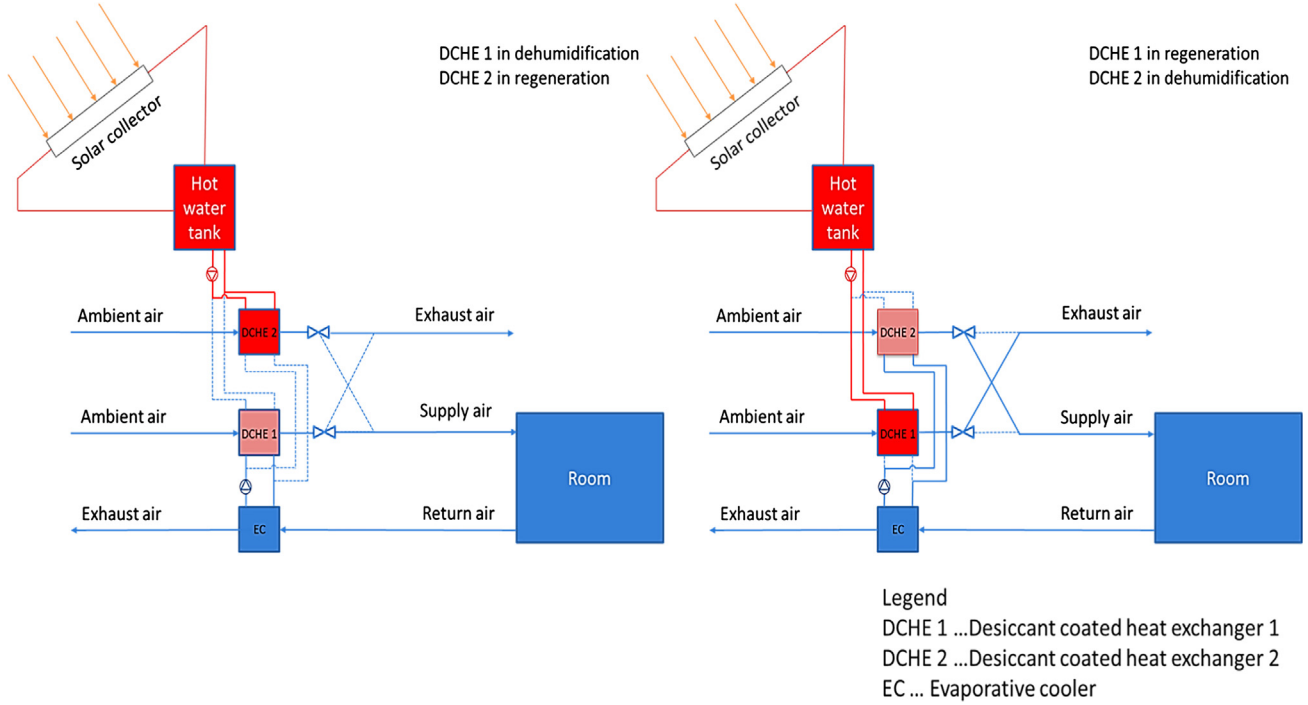

Fig. 1. Schematic figure of the solar driven desiccant coated heat exchanger cooling system, DCHE 1 in dehumidification, DCHE 2 in regeneration (left); DCHE 1 in regeneration, DCHE 2 in dehumidification (right).

Table 1
Specifications of the desiccant coated heat exchanger.

Parameter	Air Side	Water Side
Length of channel [m]	0.1	0.1
Width of channel [m]	0.03	0.03
Height of channel [m]	0.01	0.01
Number of channel [–]	10	11
Desiccant layer thickness [μm]	200	–
Heat transfer area [m^2]	0.06	0.066
Frontal cross section [m^2]	0.003	0.0033
Mass of the desiccant [g]		
Silica gel	7.88	–
Aluminium Fumarate	4.8	–
Material of the heat exchanger	Aluminium	Aluminium

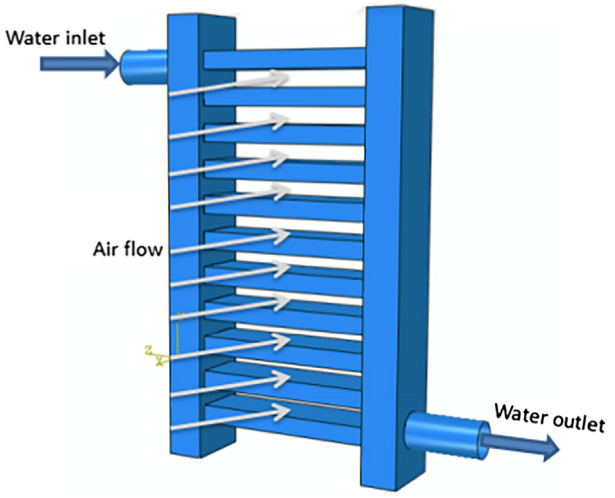

Fig. 2. Schematic of desiccant coated heat exchanger.

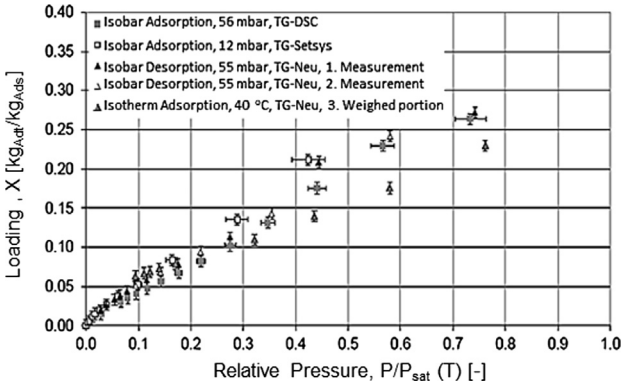

Fig. 3. Experimental Equilibrium Data for the Silica Paper composite [21].

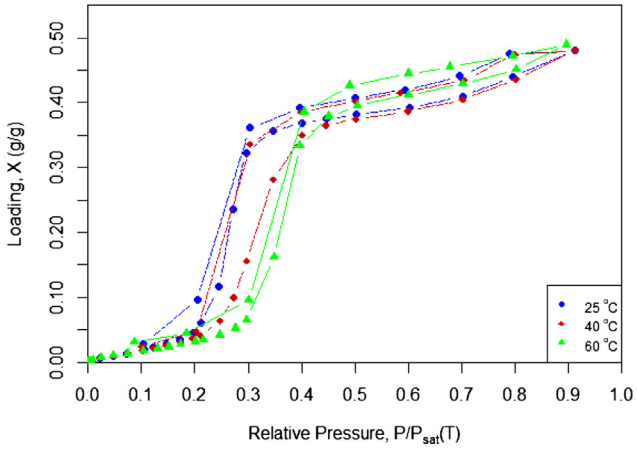

Fig. 4. Adsorption Isotherms of Aluminium fumarate for 25, 40 and 60 °C [27].

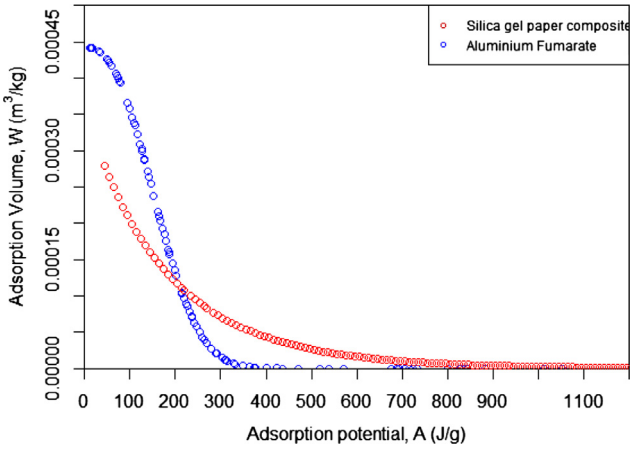

Fig. 5. Characteristic curve for silica gel paper composite and aluminium fumarate by Dubinin Astakhov Transformation.

4. Simulation model

The simulation model is structured by using the Modelica modelling language in Dymola program of version 2016, 2015-05-29. The model is solved with a differential algebraic equation multi-step solver (DASSL) using a time integration step size which is adaptive. Implicit integration algorithms with adaptive step sizes used in this solving procedure ensures the stability and provides good control of the error of the numerical solution and computational efficiency. Simulations performed within the scope of this work has a time-step of 1 s. Minimum integration step sizes for adiabatic and water-cooled models are 8.25e-06 s and 9.91e-06 s respectively. Maximum integration step sizes for adiabatic and water-cooled models are 38.4 s and 63.3 s respectively. The solution procedure of the model is shown in a flow chart in Fig. 6.

It is a physical-mathematical model which consists of three main models which are (i) the model of cooling water side, (ii) the model of the wall and (iii) the model of adsorption. The operation conditions used in the simulation are shown in Table 2.

In this study, the simulations are performed according to four different cases which are stated below:

Case-1: the heat exchanger is coated with aluminium fumarate and has cooling water channels.
Case-2: the heat exchanger is coated with silica gel and has cooling water channels.
Case-3: the heat exchanger is coated with aluminium fumarate and has no cooling water channels, in adiabatic conditions.
Case-4: the heat exchanger is coated with silica gel and has no cooling water channels, in adiabatic conditions.

The schemes of the simulation models for water-cooled and adiabatic cases are demonstrated in Figs. 7 and 8 respectively. Within the model of cooling water side, the characteristics of the water side are specified such as geometrical properties of water channels and the flow rate. The flow is described and the heat transfer coefficients are determined mathematically by considering the boundary condition of constant heat flux for simultaneously developing flow. The related Nusselt correlation is well described in the literature [30]. Pressure losses inside the water channels are neglected. The equations for the mass balance, momentum balance and energy balance are given in the nomenclature [29]:

The model of adsorption includes the geometry, the flow regimes, the heat and mass transfer coefficients, and the adsorption equilibrium related to the air side. The thermodynamic properties are determined by the equilibrium functions of the Dubinin Polanyi Theory which is properly defined in literature [21,31].

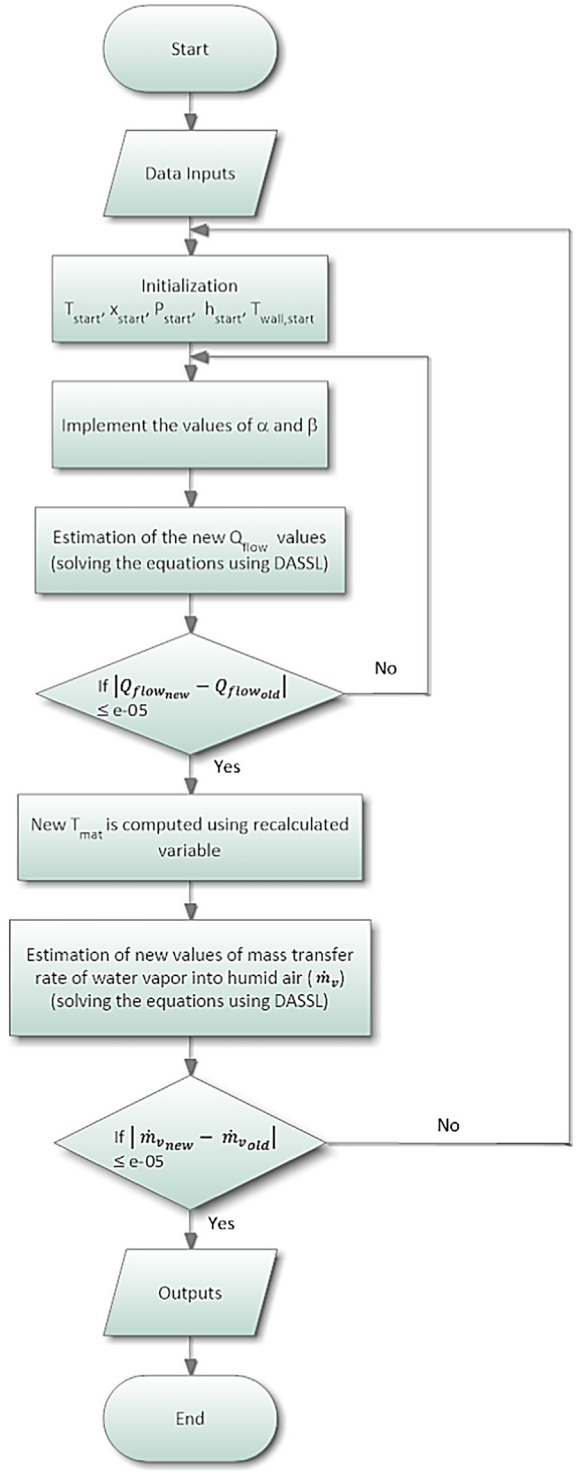

Fig. 6. Solution procedure of the simulation model.

The following assumptions have been made for the model of adsorption [21]:

- Mass and loading in the sorption layer are homogeneously distributed.
- The adsorbent is distributed uniformly and in constant layer thickness on the heat exchanger.
- The adsorbent has a thermodynamically inert behaviour. Mixing effects are completely attributed to the adsorbate.
- The mass transfer can be described by a homogeneous pseudo-gas-

Table 2
Operation conditions used in the simulation.

	Dehumidification		Regeneration	
Case 1 & 2				
	Air	Water	Air	Water
Inlet Temperature T_{in} [°C]	30	20	30	60
Humidity ratio, x_{in} [g/kg]	13	–	13	–
Inlet Relative Humidity [%]	47.82	–	47.82	–
Inlet velocity [m/s]	0.928	0.335	0.928	0.335
Mass flow rate $\dot{m}$ [kg/s]	0.001	0.1	0.001	0.1
Cycle time [s]	300	300		
Case 3 4				
		Air		Air
Inlet Temperature T_{in} [°C]		30		60
Humidity ratio, x_{in} [g/kg]		13		13
Inlet Relative Humidity [%]		47.8		10.2
Inlet velocity [m/s]		0.928		0.928
Mass flow rate $\dot{m}$ [kg/s]		0.001		0.001
Cycle time [s]		300		300

limited kinematic model.

- Heat and mass transfer are defined by local and constant heat and mass transfer coefficients.
- The thermal conductivity of the adsorbent is constant and homogeneous.
- The adsorption heat is released centrally in the adsorbent.

The wall model comprehends mainly the thermal and physical properties of wall material and adsorbent material, which are the thickness, the heat transfer area, the density, the specific heat capacity, and the thermal conductivity.

The assumptions listed below are valid for the wall model [21]:

- The mass in the walls of the heat exchanger is homogeneously distributed.
- The specific heat capacity may be accepted to be constant in the considered temperature range.
- The thickness of the heat exchanger wall is very small.
- Heat conduction through the wall is therefore approximately one-dimensional. Axial heat conduction is neglected.

The wall model takes into account the heat transfer resistance due to the contact between the adsorbent material and the wall of the heat exchanger which is applied to the heat conduction in the heat exchanger wall as well as its thermal capacity.

The heat flow between the adsorbent material and the heat transfer wall is described by means of the effective heat transfer coefficient of the contacting surfaces.

Energy balance at the heat exchanger wall is calculated based on Eqs. (11)–(14) in the nomenclature:

Inside the wall model for the adiabatic cases, a fixed heat flow is assumed to build on the wall material. Fixed heat flow allows a certain amount of heat flow rate to be introduced into a thermal system at a related inlet which is defined by Eq. (14).

In this study, a coupled heat and mass transfer model is used. The Lewis relation, which was proposed by W. K. Lewis, is the basis in this simulational analysis [32]. A Lewis number of 2, is chosen for the analysis all along the simulations. In the heat transfer analysis, the mass transfer phenomena in the adsorbent material are neglected.

The mathematical model was partially validated, that is, the heat transfer model and the mass transfer model were modeled separately and compared with experimental data available at the Fraunhofer Institute for Solar Energy Systems (ISE) [21,29]. The validation result of the model for the outlet absolute humidity of air at Le = 2 is shown in Fig. 9 [29]. It can be observed that the error of the model is in a reasonable range under the simulation conditions.

5. Performance indices

Performance of the desiccant coated heat exchanger is evaluated by the following indices, which are defined below:

Loading is defined within the simulation model by using the relation below [21]:

$$X_{eq} = f(P_{Ads}, T) \tag{17}$$

The adsorption equilibrium is uniquely determined by the relationship between the loading X_{eq}, the pressure of the adsorbent P_{Ads} and the temperature of the system T.

The loading can be also calculated as the ratio of water in the adsorbate phase (m_{Adt}) to the mass of the dry adsorbent (m_{Ads}).

$$X = \frac{m_{Adt}}{m_{Ads}} \tag{18}$$

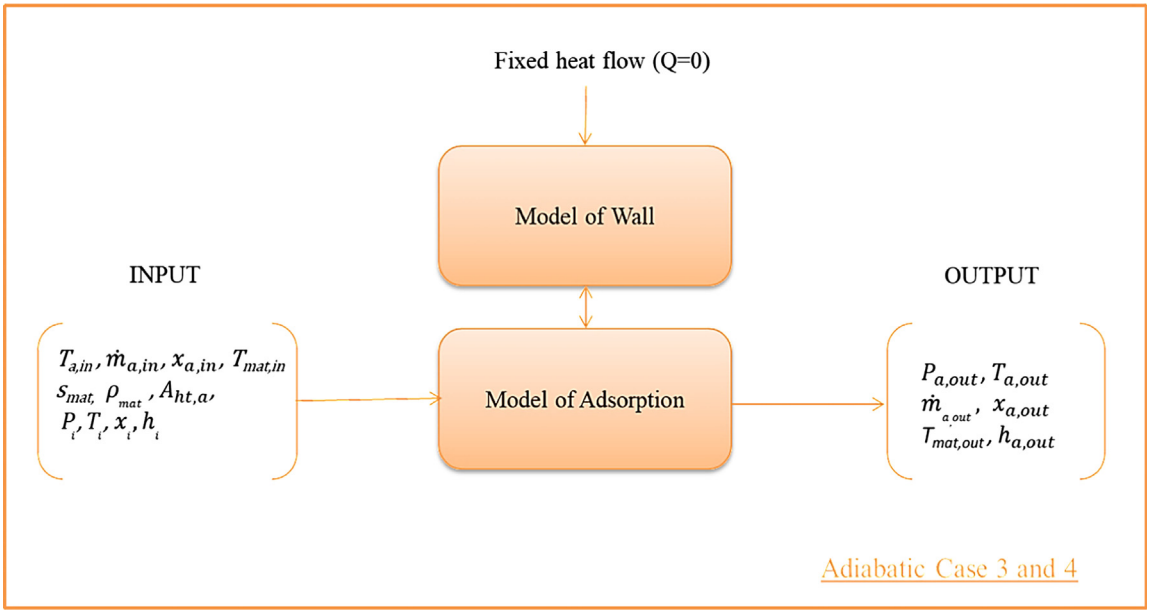

Fig. 7. Scheme of the simulation model for adiabatic cases 3 and 4.

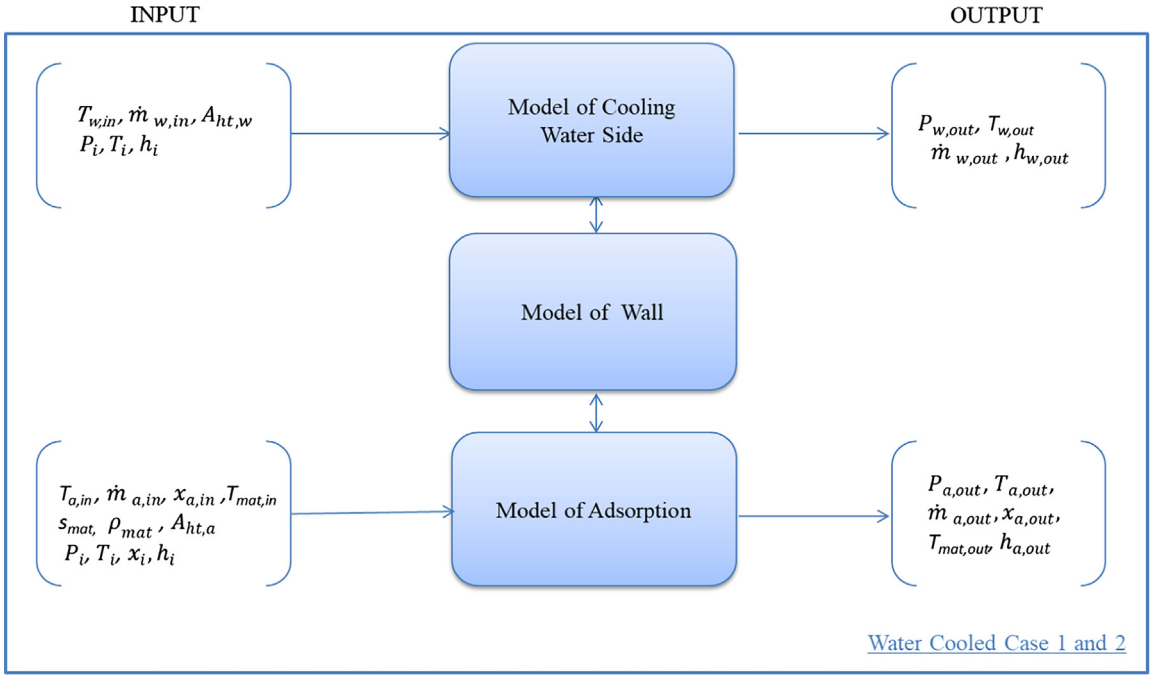

Fig. 8. Scheme of the simulation model for water cooled cases 1 and 2.

The mass transfer performance of the system is determined by the following equation which corresponds to the mass of the water in the adsorbate phase (g):

$$m_{Adt} = \beta \bullet \rho \bullet A_{ht} \bullet \int_0^{t_{de}} (x_{in} - x_{eq})dt \tag{19}$$

Dehumidification capacity is calculated by Eq. (20) [33]. In this equation, C_{de} indicates dehumidification capacity (g/s), $\dot{m}_a$ is the mass flow rate of process air (kg/s), x_{in} and x_{out} are the inlet and outlet humidity ratios of the process air (g/kg), and t_{de} is the effective dehumidification time (s).

$$C_{de} = \dot{m}_a \left(\int_0^{t_{de}} (x_{in} - x_{out})dt \right) / t_{de} \tag{20}$$

Regeneration capacity can be defined based on the equation of moisture removal performance of regeneration process [34]. In this equation, C_{rg} indicates regeneration capacity (g/s), and t_{rg} is the effective regeneration time (s).

$$C_{rg} = \dot{m}_a \left(\int_0^{t_{rg}} (x_{in} - x_{out})dt \right) / t_{rg} \tag{21}$$

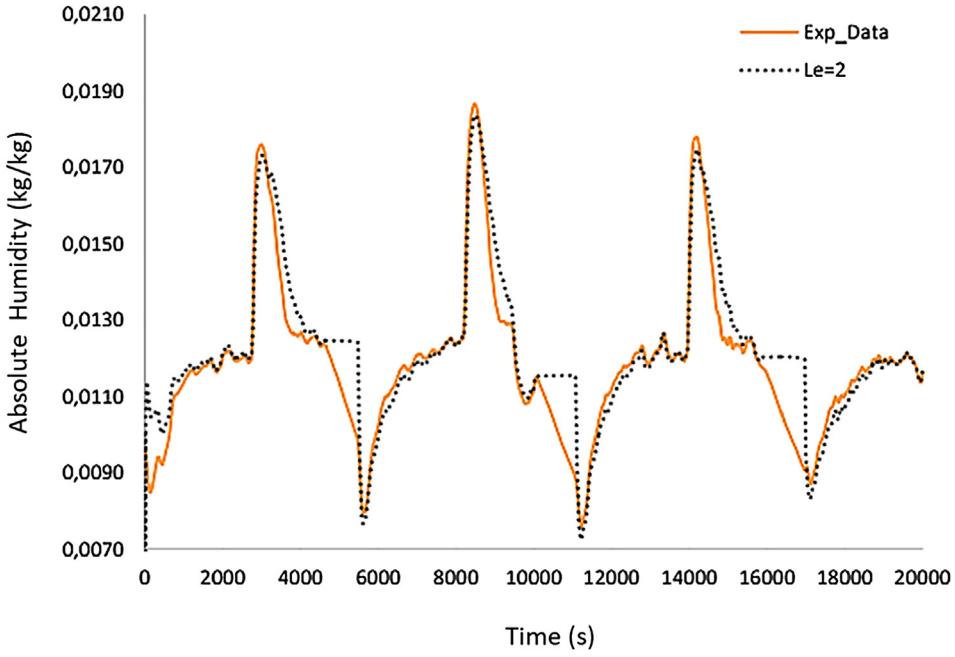

Fig. 9. Validation result of the model for the outlet absolute humidity of air at Le = 2 [29].

6. Results and discussion

The heat exchanger used in this simulation study, had a 0.06 m^2 heat transfer area and 200 µm area desiccant layer thickness. Depending on the adsorbent material properties and coating techniques, the total mass of adsorbent is different; for silica gel the total mass is 7.9 g while for aluminium fumarate is 4.8 g. In a real application, the total mass of the adsorbent material is highly dependent on the coating technique and the material itself.

For the aluminium fumarate coated heat exchanger, the volume flow rates, the inlet air temperature, and the inlet humidity ratio values are the same as for silica gel coated heat exchanger, however, the coating technique conditions are different. Since aluminium fumarate is a highly porous material, the estimated density is only 400 kg/m^3 in the conservative and realistic case [29]. This corresponds to a total mass of aluminium fumarate of 4.792 g on the surface of the heat exchanger.

The performance of the sorptive heat exchanger using silica gel-paper-composite as adsorbent material is analyzed. For these analyses, the adsorbent layer thickness over the surface of the heat exchanger and the density of the adsorbent layer are defined as 200 µm and 658 kg/m^3 respectively. [20]. The total mass of silica gel calculated on the surface of the heat exchanger is 7.883 g.

The mass flow rate of air is 0.001 kg/s and it is constant during all cycles. The mass flow rate for the cooling water is 0.1 kg/s and stays constant during all cycles. In the dehumidification (adsorption) and regeneration cycles of the water-cooled cases 1 and 2, inlet relative humidity of the process air is 47.8%, whereas, for regeneration (desorption) cycles, inlet relative humidity of the process air is 10.2% related to the adiabatic cases 3 and 4. For the water-cooled cases 1 and 2, the inlet process air temperature (ambient air) for the adsorption and desorption is 30 °C. For the adiabatic cases 3 and 4, inlet process air temperature for the adsorption is 30 °C and for the desorption 60 °C. Relative humidity and temperature values of inlet process air of the sixth cycle are shown in Table 2.

The results of the simulations are shown in Figs. 10–14.

In the dehumidification cycles, for the water-cooled cases Case 1 and 2, the heat transfer coefficient is 31.9 W/m^2 K. In the regeneration cycles, it is 33.3 W/m^2 K. In adiabatic cases 3–4, the heat transfer coefficients are ranging between 32.2 and 33.5 W/m^2 K. For both of the adiabatic cases, they reach their highest values at the end of regeneration and have their lowest values at the end of dehumidification. As mass transfer coefficients are correlated with heat transfer coefficients and Lewis relation is used, mass transfer coefficients show a similar response to the heat transfer coefficients. The mass transfer coefficients used in the water-cooled and adiabatic cases are 0.017 and 0.019 m/s in the dehumidification and regeneration cycles respectively.

Outlet air temperatures (supply air and exhaust air) of the cases 1–4 are shown in Fig. 10. In the water-cooled cases 1–2, the outlet air temperatures are 50 °C, and 24 °C in the regeneration and dehumidification respectively. In the water-cooled cases 1–2, the temperatures during the dehumidification and regeneration phases have a tendency to stay nearly constant. In the adiabatic cases 3–4, the outlet air temperatures decrease along the dehumidification phase and increase along the regeneration phase. The average outlet air temperatures of cases 3–4 are 49 °C, and 42 °C in the regeneration and dehumidification respectively.

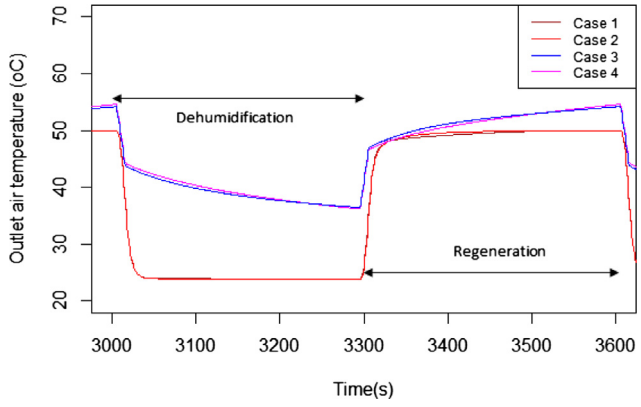

Fig. 10. Outlet air temperature(°C) of the sixth cycle (**Case 1**: aluminium fumarate coating, wc, **Case 2**: composite silica gel coating, wc; **Case 3**: aluminium fumarate coating, adi, **Case 4**: composite silica gel coating, adi).

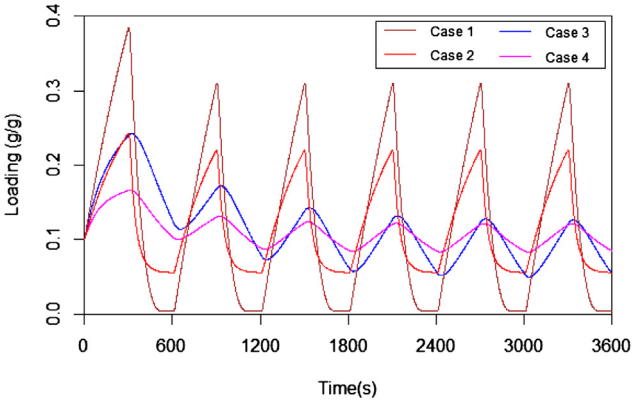

Fig. 11. Loading curve (g_{Adt}/g_{Ads}) of the four cases along 6 cycles (**Case 1**: aluminium fumarate coating, wc, **Case 2**: composite silica gel coating, wc; **Case 3**: aluminium fumarate coating, adi, **Case 4**: composite silica gel coating, adi).

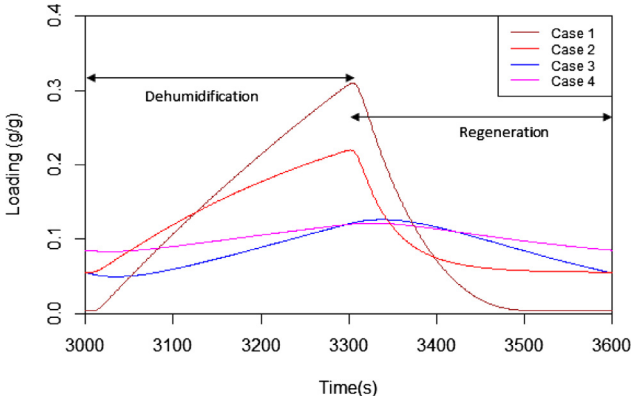

Fig. 12. Loading curve (g_{Adt}/g_{Ads}) of the sixth cycle.

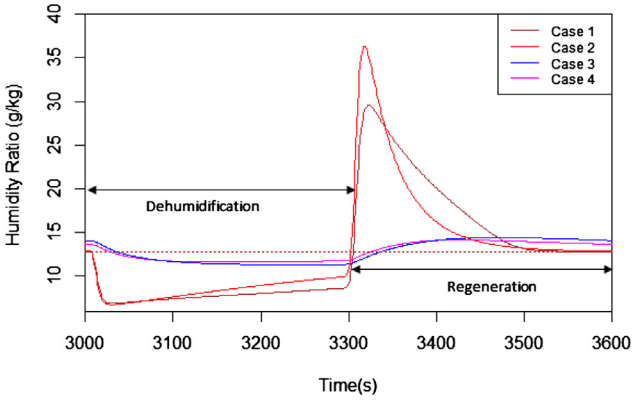

Fig. 13. Outlet and inlet humidity ratio of the process air (g/kg) along the sixth cycle.

Loading curves related to the water-cooled and adiabatic cases are shown in Figs. 11 and 12. In case-1, the maximum loading at the first cycle is 0.385, it drops to 0.31 at the second cycle and stays nearly

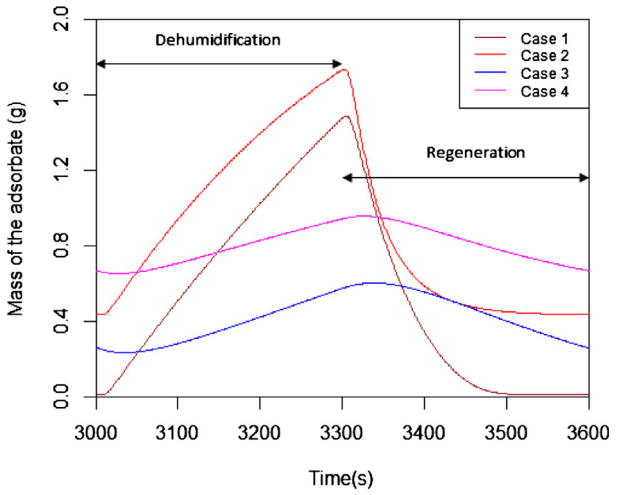

Fig. 14. Mass of the adsorbate (g) of the sixth cycle (**Case 1**: aluminium fumarate coating, wc, **Case 2**: composite silica gel coating, wc; **Case 3**: aluminium fumarate coating, adi, **Case 4**: composite silica gel coating, adi).

constant along the following 4 cycles. In case-2, the maximum loading at the first cycle is 0.243 whereas the last 5 cycles it decreases 9% and is in a stable condition. In the adiabatic cases 3–4, the maximum loading falls sharply after the first cycle, In case-3, it becomes stable after 3 cycles. In case 4, the maximum loading becomes almost constant after 2 cycles. Maximum loading values for case 1 is greater than that of case 3 by a factor of 1.3, and maximum loading in case-2 is 43% greater than case 4 at the last three cycles of the four cases. Maximum loading value of the case 1 is 41% greater than that of case 2.

The outlet and inlet humidity ratios of the process air (g/kg) for the water-cooled and adiabatic cases are given in Fig. 13. For the Case 1, the outlet humidity ratio during cycles is ranging between 6.89 and 29.57 g/kg whereas for the Case 2, it becomes 6.74–36.33 g/kg. For the adiabatic cases, in Case 3, the outlet humidity range is between 11.32 and 14.42 g/kg. In case 4, the outlet humidity ratio range is between 11.62 and 14.14 g/kg. Overall, Case 2 has the highest outlet humidity ratios.

Mass of the adsorbate removed from the air at the cycle 6 is demonstrated in Fig. 14. Composite silica gel coated heat exchanger (Case-1), has the highest adsorbate mass of 1.7 g which is 17% greater than aluminium fumarate coated heat exchanger (Case-2). Maximum adsorbate masses are nearly 0.6 and 1 g for the cases 3–4, respectively. In the adiabatic cases 3–4, composite silica gel coated heat exchanger enables to remove 66.6% higher adsorbate mass than the aluminium fumarate coated heat exchanger. Water-cooled case-2 shows 70% higher adsorbate removal compared to the adiabatic case-4. Water-cooled case -1, shows 1.4 factor higher adsorbate removal performance compared to the adiabatic case-3.

Performance indices of the system computed for the simulations are given in Table 3.

7. Conclusions

Solid desiccant coated heat exchangers have significant role in the evolution of new designs in desiccant cooling systems. The type of the solid desiccant is a critical factor in the performance as well as the design of the heat exchanger. Silica gel has found a widescale use in these heat exchangers. Recently, some researchers focused their attention on the metal organic frameworks (MOFs) due to its superior properties. Therefore, in this paper, a simulation study has been conducted for the comparison of the performances of heat exchangers coated with silica gel and aluminium fumarate which are configured in four different cases. Performance of the heat exchangers is assessed by using the performance indices. Loading, humidity ratio, heat and mass transfer coefficients, dehumidification, and regeneration capacities are determined for 6 cycles.

The following conclusions have been derived from the above work:

(i) Compared to silica gel paper composite coated heat exchanger, aluminium fumarate coated heat exchanger shows 8% higher dehumidification capacity and 11% higher regeneration capacity under the same specified operation conditions.
(ii) Loading value of aluminium fumarate coated heat exchanger for the water-cooled case is 41% higher than the loading value of silica gel coated heat exchanger. However, the mass of the silica gel paper composite adsorbent is 64% higher than that of aluminium fumarate for the same coating thickness of 0.2 mm.
(iii) Heat and mass transfer coefficients show nearly constant behaviour for the water-cooled case which is the consequence of constant medium (air) temperature and density. For the adiabatic cases, they tend to fall during dehumidification phase due to the decrease in medium temperature and increase in density whereas it

Table 3
Performance parameters computed for the simulation.

Parameters	1. cycle	2. cycle	3.cycle	4. cycle	5. cycle	6.cycle
Case 1						
Maximum loading, X (g_{Adt}/g_{Ads})	0.385	0.310	0.310	0.310	0.310	0.310
Maximum mass of adsorbate, (g)	1.846	1.487	1.487	1.487	1.487	1.487
Dehumidification capacity, C_{de} (g/s)	0.00450	0.00475	0.00460	0.00443	0.00425	0.00407
Regeneration capacity, C_{rg}(g/s)	0.0060	0.0048	0.0046	0.0044	0.0042	0.0041
Case 2						
Maximum loading, X (g_{Adt}/g_{Ads})	0.243	0.220	0.220	0.220	0.220	0.220
Maximum mass of adsorbate, (g)	1.92	1.734	1.734	1.734	1.734	1.734
Dehumidification capacity, C_{de} (g/s)	0.00372	0.00423	0.00412	0.00399	0.00386	0.00374
Regeneration capacity, C_{rg}(g/s)	0.0048	0.0042	0.0041	0.0040	0.0039	0.0037
Case 3						
Maximum loading, X (g_{Adt}/g_{Ads})	0.242	0.172	0.142	0.131	0.127	0.126
Maximum mass of adsorbate, (g)	1.163	0.824	0.683	0.631	0.611	0.605
Dehumidification capacity, C_{de} (g/s)	0.0022	0.0006	0.0008	0.0008	0.0007	0.00069
Regeneration capacity, C_{rg}(g/s)	0.00175	0.00128	0.00100	0.00085	0.00075	0.00066
Case 4						
Maximum loading, X (g_{Adt}/g_{Ads})	0.166	0.131	0.1235	0.1218	0.1214	0.1214
Maximum mass of adsorbate, (g)	1.313	1.04	0.975	0.961	0.959	0.959
Dehumidification capacity, C_{de} (g/s)	0.00172	0.0006	0.0008	0.0008	0.0007	0.00066
Regeneration capacity, C_{rg} (g/s)	0.00159	0.00100	0.00083	0.00075	0.00069	0.00063

tends to rise during regeneration phase due to the decrease in the density of the medium.

(iv) In the water-cooled case, removal of the adsorbate is more than 70% higher compared to adiabatic case.

(v) Mass of the adsorbate removed with silica gel coated heat exchanger is 17% higher than that of aluminium fumarate coated heat exchanger in water-cooled cases under the same specific operation conditions. In the adiabatic cases, a composite silica gel coated heat exchanger has a capability to remove 66.6% higher adsorbate mass than the aluminium fumarate coated heat exchanger.

Motivation of a future work could be implementation of different MOFs (MIL-101, CAU10-H, etc.) to the model and extension of the model in order to simulate the performance of a solar powered or waste heat driven solid desiccant cooling system.

Acknowledgements

The authors acknowledge the financial support from TÜBİTAK (fellowship of 2214-A), which enabled Türkan Üçok Erkek to perform measurements and simulations at the Fraunhofer Institute for Solar Energy Systems, ISE. The authors also acknowledge the financial support from the German Federal Ministry of Education and Researchsps:id::GS1||sponsor-id::http://dx.doi.org/10.13039/501100009245 (BMBF) for the Optimat Project (FKZ 03SF0492A).

Appendix A. Supplementary material

Supplementary data associated with this article can be found, in the online version, at https://doi.org/10.1016/j.applthermaleng.2018.06.012.

Nomenclature

A_{ht}	*heat transfer area*	*[m^2]*
A	adsorption potential	[J/g]
C	capacity	[g/s]
c_p	specific heat capacity	[J/kg·K]
H	enthalpy	[J]
h	specific enthalpy	[J/g]
m	mass	[kg]
$\dot{m}$	mass flow rate	[kg/s]
$\dot{m}_{mr}$	moisture removal rate	[g/s]
P	pressure	[Pa]
Q	heating power	[kW]
$\dot{Q}$	heat flux	[W]
s	thickness	[m]
T	temperature	[°C]
t	time	[s]
U	internal energy	[J]
W	adsorption volume	[m^3]
X	loading	[g/g]
x	humidity ratio	[g/kg]

Greek Symbols

α	*heat transfer coefficient*	*[W/m^2·K]*
β	*mass transfer coefficient*	*[m/s]*
ρ	*density*	*[kg·m^{-3}]*
λ	*thermal conductivity*	*[W/m·K]*

Subscripts

a	air
Ads	adsorbent phase
Adt	adsorbate phase
c	cooling
cf	core flow
ct	contact
de	dehumidification
eq	equilibrium
hex	heat exchanger
i	initial
in	inlet
m	average
mat	adsorbent material
rg	regeneration
s	source
sat	saturation
out	outlet
v	*vapor*
w	water

Abbreviations

DASSL	Differential algebraic system solver
DCHE	Desiccant coated heat exchanger
wc	water-cooled
adi	adiabatic

Equations	Used in the Simulation Model	Equation	
(1)	Mass balance, water side $\frac{d(m_w)}{dt} = \dot{m}_{w,out} - \dot{m}_{w,in}$	(8)	Momentum balance, air side: $P_{a,in} = P_{a,out}$
(2)	Momentum balance, water side: $P_{w,in} = P_{w,out}$	(9)	Energy balance, adsorptive material $m_{Ads} \cdot c_{pAds} \frac{d(T_{mat})}{dt} = \frac{d(m_w)}{dt} h_{Ads} - \alpha \cdot (T_{mat} - T_m) + \dot{Q}_{Ads}$
(3)	Energy balance, water side: $\frac{d(U_w)}{dt} = \dot{H}_{w,out} - \dot{H}_{w,in} + \dot{Q}_w$	(10)	Energy balance, air side $\frac{d(U_a)}{dt} = \dot{H}_{a,out} - \dot{H}_{a,in} + \dot{Q}_a$
(4)	Mass Balance, adsorptive material: $\frac{d(m_{Adt})}{dt} = \beta \cdot \rho \cdot A_{ht} \cdot (x_{in} - x_{eq})$	(11)	$\dot{Q}_{ct} = \alpha_{ct} \cdot A_{ht} (T_{Ads,cf} - T_{hex})$
(5)	$x_{eq} = 0.622 \frac{P_S}{P - P_S}$	(12)	$\dot{Q}_{ct} = \dot{Q}_{hex,a}$
(6)	Mass balance, air side: $\frac{d(m_a)}{dt} = \dot{m}_{a,out} - \dot{m}_{a,in} + m_{Adt}$	(13)	$m_{hex} \cdot c_{phex} \frac{d(T_{hex})}{dt} = \dot{Q}_{hex,a} + \dot{Q}_{hex,cf} = \frac{\lambda_{hex}}{s_{hex}/2} \cdot A \cdot (T_{hex,a} - T_{hex}) + \frac{\lambda_{hex}}{s_{hex}/2} \cdot A \cdot (T_{hex,b} - T_{hex})$
(7)	$\frac{d(m \cdot X_w)}{dt} = \dot{m}_{w,in} \cdot X_w + \dot{m}_{w,out} \cdot X_w + m_{Adt}$	(14)	Heat flow: $Q_{in} = Q_{flow} \cdot (1 - \alpha \cdot (T_{in} - T_i))$

References

[1] T. Sookchaiya, V. Monyakul, S. Thepa, Assessment of the thermal environment effects on human comfort and health for the development of novel air conditioning system in tropical regions, Energy Build. 42 (2010) 1692–1702.

[2] Building Design, Active HVAC Systems, Humidity Control, accessed August 14, 2017, < https://sustainabilityworkshop.autodesk.com/buildings/humidity-control > .

[3] C.E.L. Nóbrega, N.C.L. Brum, Desiccant-Assisted Cooling, Fundamentals and Applications, London, 2014.

[4] K. Fathalah, S.E. Aly, Study of a waste heat driven modified packed desiccant bed dehumidifier, Energy Convers. Manage. 37 (1996) 457–471.

[5] Y. Zheng, W. Yuan, H. Wang, X. Yuan, Experiments on dynamic dehumidification of internally cooling compact solid dehumidifier, J Beijing Univ. Aeronaut Astronaut 32 (2006) 1100–1103.

[6] Y. Weixing, Z. Yi, L. Xiaoru, Y. Xiugan, Study of a new modified cross-cooled compact solid desiccant dehumidifier, Appl. Therm. Eng. 28 (2008) 2257–2266.

[7] T.S. Ge, Y.J. Dai, R.Z. Wang, Y. Li, Feasible study of a self-cooled solid desiccant cooling system based on desiccant coated heat exchanger, Appl. Therm. Eng. 58 (2013) 281–290.

[8] C. Bongs, A. Morgenstern, Y. Lukito, H.M. Henning, Advanced performance of an open desiccant cycle with internal evaporative cooling, Sol. Energy 104 (2014) 103–114.

[9] L.M. Hu, T.S. Ge, Y. Jiang, R.Z. Wang, Performance study on composite desiccant material coated fin-tube heat exchangers, Int. J. Heat Mass Transfer 90 (2015) 109–120.

[10] T.S. Ge, Y.J. Dai, R.Z. Wang, Performance study of silica gel coated fin-tube heat exchanger cooling system based on a developed mathematical model, Energy Convers. Manage. 52 (2011) 2329–2338.

[11] Y.D. Tu, R.Z. Wang, T.S. Ge, X. Zheng, Comfortable, high-efficiency heat pump with desiccant-coated, water-sorbing heat exchangers, Sci. Rep. 7 (2017) 40437.

[12] S.J. Oh, K.C. Ng, W. Chun, K.J.E. Chua, Evaluation of a dehumidifier with adsorbent coated heat exchangers for tropical climate operations, Energy 137 (2017) 441–448.

[13] Y. Jiang, T.S. Ge, R.Z. Wang, L.M. Hu, Experimental investigation and analysis of composite silica-gel coated fin-tube heat exchangers, Int. J. Refrig. 51 (2015) 169–179.

[14] N. Enteria, H. Yoshino, A. Satake, A. Mochida, R. Takaki, R. Yoshie, S. Baba, Development and construction of the novel solar thermal desiccant cooling system incorporating hot water production, Appl. Energy 87 (2010) 478–486.

[15] T.S. Ge, Y.J. Dai, Y. Li, R.Z. Wang, Simulation investigation on solar powered desiccant coated heat exchanger cooling system, Appl. Energy 93 (2012) 532–540.

[16] K.F. Fong, T.T. Chow, C.K. Lee, Z. Lin, L.S. Chan, Advancement of solar desiccant cooling system for building use in subtropical Hong Kong, Energy Build. 42 (12) (2010) 2386–2399.

[17] N. Enteria, H. Awbi, H. Yoshino, Desiccant Heating, Ventilating, and Air-Conditioning Systems, Springer, Singapore, ISBN 978-981-10-3047-5, 2017.

[18] L.W. Wang, R.Z. Wang, R.G. Oliveira, A review on adsorption working pairs for refrigeration, Renew. Sustain. Energy Rev. 13 (2009) 518–534.

[19] F. Jeremias, Synthesis and Characterization of Metal-Organic Frame-works for Heat Transformation Applications, Heinrich-Heine-Universitat, Düsseldorf, Dissertation, 2014.

[20] M.M. Dubinin, V.A. Astakhov, Description of Adsorption Equilibria of Vapors on Zeolites over Wide Ranges of Temperature and Pressure, in: Gould, R.F. (Hrsg.): Advances in Chemistry. American Chemical Society, 1971, 102.

[21] C. Bongs, Experimentelle und mathematisch-numerische Untersuchung von Verdunstungsgekuhlten, sorptive beschichteten Warmeubertragern für die Luftentfeuchtung und kühlung, Technische Universitat Berlin, Dissertation, 2013.

[22] F. Rouquerol, J. Rouquerol, K. Sing, Adsorption by Powders and Porous Solids Principles, Methodology and Applications, Academic Press, 1999.

[23] D.D. Do, Adsorption Analysis: Equilibria and Kinetics, Imperial College Press, 1998.

[24] Y. Aristov, Novel materials for adsorptive heat pumping and storage: screening and nanotailoring of sorption properties, J. Chem. Eng. Jpn. 40 (13) (2007) 1242–1251.

[25] P. Küsgens, M. Rose, I. Senkovska, H. Frode, A. Henschel, S. Siegle, S. Kaskel, Characterization of metal-organic frameworks by water adsorption, Microporous Mesoporous Mater. 120 (3) (2009) 325–330.

[26] S.K. Henninger, F. Jeremias, H. Kummer, C. Janiak, MOFs for use in adsorption heat pump processes, Eur. J. Inorg. Chem. 16 (2012) 2625–2634.

[27] F. Jeremias, D. Fröhlich, C. Janiak, S.K. Henninger, Advancement of sorption-based heat transformation by a metal coating of highly-stable, hydrophilic aluminium fumarate MOF, RSC Adv. 46 (2014) 24073–24082.

[28] H. Kummer, F. Jeremias, A. Warlo, G. Füldner, D. Fröhlich, C. Janiak, R. Gläser, S.K. Henninger, A functional full-scale heat exchanger coated with aluminum fumarate metal − organic framework for adsorption heat transformation, Ind. Eng. Chem. Res. 56 (2017) 8393–8398.

[29] J. Galan, Evaluation of Water-Cooled Sorptive Heat Exchanger on the Basis of Novel Adsorption Materials for Air Conditioning, Technical University Berlin, Master Thesis, 2016.

[30] R.K. Shah, D. Sekulic, Fundamentals of Heat Exchanger Design, John Wiley Sons, 2003.

[31] T. Núñez, Charakterisierung und Bewertung von Adsorbentien für Wärmetransformationsanwendungen, Albert-Ludwigs-Universität Freiburg, Dissertation, 2001.

[32] J.C. Kloppers, D.G. Kroger, The Lewis factor and its influence on the performance prediction of wet-cooling towers, Int. J. Therm. Sci. 44 (2005) 879–884.

[33] X. Zheng, T.S. Ge, Y. Jiang, R.Z. Wang, Experimental study on silica gel-LiCl composite desiccants for desiccant coated heat exchanger, Int. J. Refrig. 51 (2015) 24–32.

[34] Y. Zhao, Y.J. Dai, T.S. Ge, H.H. Wang, R.Z. Wang, A high performance desiccant dehumidification unit using solid desiccant coated heat exchanger with heat recovery, Energy Build. 116 (2016) 583–592.